J|A|C|S ARTICLES

Published on Web 08/12/2009

Improving Electrocatalysts for O_2 Reduction by Fine-Tuning the Pt−Support Interaction: Pt Monolayer on the Surfaces of a $Pd_3Fe(111)$ Single-Crystal Alloy

Wei-Ping Zhou,[†] Xiaofang Yang,[‡] Miomir B. Vukmirovic,[†] Bruce E. Koel,[‡] Jiao Jiao,[§] Guowen Peng,[§] Manos Mavrikakis,[§] and Radoslav R. Adzic*[,†]

Chemistry Department, Brookhaven National Laboratory, Upton, New York 11973, Chemistry Department, Lehigh University, 9 West Packer Avenue, Bethlehem, Pennsylvania 18015, and Department of Chemical & Biological Engineering, University of Wisconsin-Madison, Madison, Wisconsin 53706

Received May 15, 2009; E-mail: adzic@bnl.gov

Abstract: We improved the effectiveness of Pt monolayer electrocatalysts for the oxygen-reduction reaction (ORR) using a novel approach to fine-tuning the Pt monolayer interaction with its support, exemplified by an annealed $Pd_3Fe(111)$ single-crystal alloy support having a segregated Pd layer. Low-energy ion scattering and low-energy electron diffraction studies revealed that a segregated Pd layer, with the same structure as Pd (111), is formed on the surface of high-temperature-annealed $Pd_3Fe(111)$. This Pd layer is considerably more active than Pd(111); its ORR kinetics is comparable to that of a Pt(111) surface. The enhanced catalytic activity of the segregated Pd layer compared to that of bulk Pd apparently reflects the modification of Pd surface's electronic properties by underlying Fe. The $Pd_3Fe(111)$ suffers a large loss in ORR activity when the subsurface Fe is depleted by potential cycling (i.e., repeated excursions to high potentials in acid solutions). The $Pd_3Fe(111)$ surface is an excellent substrate for a Pt monolayer ORR catalyst, as verified by its enhanced ORR kinetics on $PT_{ML}/Pd/Pd_3Fe(111)$. Our density functional theory studies suggest that the observed enhancement of ORR activity originates mainly from the destabilization of OH binding and the decreased Pt−OH coverage on the $Pt/Pd/Pd_3Fe(111)$ surface. The activity of $Pt_{ML}/Pd(111)$ and Pt(111) is limited by OH removal, whereas the activity of $Pt_{ML}/Pd/Pd_3Fe(111)$ is limited by the O−O bond scission, which places these two surfaces on the two sides of the volcano plot.

1. Introduction

Polymer electrolyte membrane fuel cells (PEMFCs) are considered a potential power source for automotive and residential applications.[1] However, the promise of their widespread application is seriously hindered by the necessarily high content of Pt in the cathode catalysts and the slow kinetics of oxygen reduction reaction (ORR) on Pt-based catalysts.[2,3] New catalysts are needed that reduce considerably the Pt content while affording the possibility of enhanced catalytic activity. Accordingly, studies of Pt monolayer (Pt_{ML}) catalysts on well-ordered model electrodes can help us in achieving a fundamental understanding of the relationship between their activity and the surface's electronic and chemical properties and so help in designing new catalysts. In our previous studies[4] of the ORR on Pt monolayers supported on well-ordered electrodes, viz., Au(111), Pd(111), Rh(111), Ir (111), and Ru(0001), we found that a Pt_{ML} on Pd(111) had higher ORR activity than Pt(111). Further assessments with nanoparticle supports demonstrated[4−8] the potential of this approach for resolving the problems of high Pt content and low efficiency in conventional Pt electrocatalysts.[4,7] In addition, Pt_{ML} studies open very interesting possibilities for designing surfaces with specific catalytic properties by using substrates with selected electronic properties. Here, we describe a straightforward way of designing more active catalysts for the ORR by employing the surfaces of single-crystal alloys to manipulate the substrate's effect and increase the activity of Pt monolayers. We also identified the mechanism responsible for the enhancement of the ORR activity of Pd alloy surfaces.

Our early studies,[7,9−12] and recently published data by others,[13−16] show that the ORR activity for Pd−M (M = Co, Fe, or Ti) alloys is comparable to or slightly better than that of the commercial Pt catalysts, thereby confirming their promise as candidates to replace Pt for the ORR. However, we cannot directly establish the mechanism of their enhanced ORR activity

[†] Brookhaven National Laboratory.
[‡] Lehigh University.
[§] University of Wisconsin-Madison.

(1) Jacobson, M. Z.; Colella, W. G.; Golden, D. M. *Science* **2005**, *308*, 1901.
(2) Adzic, R. R. In *Electrocatalysis*; Lipkowski, J., Ross, P. N., Eds.; Wiley: New York, 1998; p 197.
(3) Gasteiger, H. A.; Kocha, S. S.; Sompalli, B.; Wagner, F. T. *Appl. Catal., B* **2005**, *56*, 9.
(4) Zhang, J.; Vukmirovic, M. B.; Xu, Y.; Mavrikakis, M.; Adzic, R. R. *Angew. Chem., Int. Ed.* **2005**, *44*, 2132.
(5) Zhang, J.; Mo, Y.; Vukmirovic, M. B.; Klie, R.; Sasaki, K.; Adzic, R. R. *J. Phys. Chem. B* **2004**, *108*, 10955.
(6) Sasaki, K.; Zhang, L.; Adzic, R. R. *Phys. Chem. Chem. Phys.* **2008**, *10*, 159.
(7) Adzic, R. R.; Zhang, J.; Sasaki, K.; Vukmirovic, M. B.; Shao, M. H.; Wang, J. X.; Nilekar, A. U.; Mavrikakis, M.; Valerio, J. A.; Uribe, F. *Top. Catal.* **2007**, *46*, 249.
(8) Vukmirovic, M. B.; Liu, P.; Muckerman, J. T.; Adzic, R. R. *J. Phys. Chem. C* **2007**, *111*, 15306.

10.1021/ja9039746 CCC: $40.75

from studies of high surface area catalysts. Proposed ways to do so include modifying the electronic properties of Pd in the surface-segregated layer[9,11,17−19] or exploring the synergistic effect between Pd and the second metal.[13−15] The segregation of Pd to the surfaces of alloys was observed in ultrahigh vacuum (UHV) studies of some Pd−bimetallic systems.[20−22] Electronic structure calculations[23,24] predict that Pd has strong surface segregation tendency, for instance, in a Pd/Fe system. This segregated Pd surface layer that has different electronic properties from pure Pd[17] was considered to be the key factor responsible for the enhanced ORR activity on Pd−M alloys.[9,11,12,18] Nevertheless, direct answers are lacking for questions on how the chemical surface's compositions of Pd change with temperature in Pd−bimetallic systems and how the electronic properties of segregation-induced Pd surfaces affect catalytic activity.

Numerous UHV studies revealed that metal monolayers supported on various metal substrates exhibit chemical and catalytic properties very different from those of the surfaces of the individual metals,[25−27] which was also confirmed in several electrocatalytic studies.[4,28,29] It is generally accepted that changes in the electronic properties of metal overlayers, particularly shifts of the weighted d-band center resulting from the cumulative contributions of lattice strain and ligand effect, are likely to account for this phenomenon.[7,30−35] More importantly herein, studies of a Pt_{ML} supported on a well-ordered Pd surface with electronic properties different from those of a Pd pure phase might well advance our understanding of the Pt_{ML}−substrate interaction, a key factor determining the Pt_{ML}'s catalytic properties.

In the present work, we used a combination of experimental and theoretical studies, including rotating ring disk electrode (RRDE), low-energy ion scattering (LEIS), low-energy electron diffraction (LEED), and density functional theory (DFT) calculations, to gain a fundamental understanding of the origin of the enhanced ORR activity of the Pd_3Fe alloy. We demonstrated that a segregated Pd surface layer on $Pd_3Fe(111)$, formed after high-temperature annealing, exhibits electrochemical behavior different from that of a Pd(111) electrode, whereas its ORR activity is comparable to that of a Pt(111) electrode. To assess the effect of Fe in subsurface layers on the chemical and electrocatalytic properties of a Pd electrode's surface, we compared the electrochemical behavior and also the ORR activity of the annealed and electrochemically polished $Pd_3Fe(111)$ surfaces. Our DFT calculations substantiate the different electronic and chemical properties of the segregation-induced Pd surface layer from bulk Pd.[17] The results, providing information to advance our understanding of fine-tuning Pt monolayers−substrate interaction and supported by theoretical insights on these mechanisms, are expected to help with optimizing the Pt_{ML} ORR electrocatalytic activity.

2. Methods

2.1. Surface Preparation and Characterization in UHV. Disk-shaped $Pd_3Fe(111)$, Pd(111), and Pt(111) electrodes, 6 mm in diameter and 4 mm thick, were obtained from Metal-Crystal and Oxide, Cambridge, England. The crystal's surfaces were prepared in an ultrahigh vacuum chamber equipped with facilities for LEIS, XPS, and LEED, with a background pressure of 2×10^{-10} Torr. The $Pd_3Fe(111)$ surface was cleaned by several cycles of bombardment with Ar ions and subsequent annealing in a vacuum to 1200 K. Surface cleanliness was monitored routinely by XPS; our criterion for a clean surface was no detection of impurities above 0.5 atom %. The surface composition of clean $Pd_3Fe(111)$ was determined from LEIS spectra acquired with 1 keV He^+ ions at a beam current of ~10 nA and a scan time of 75 s spectrum^{-1}. The ions were incident at 40° from the surface plane, and the scattering angle was 130°. Details were reported earlier, using an equation to calculate the Pd and Fe surface atomic fractions.[36]

2.2. Electrochemical Measurements. Before electrochemical measurements, the single crystals $Pd_3Fe(111)$ and Pd(111) were annealed at 1200 K using an induction heating while passing[8] over them in a quartz tube a stream of high-purity Ar gas (Matheson, 99.9999%). Thereafter, they were cooled close to room temperature either at the same atmosphere for Pd(111) or adding less than 2% of H_2 in Ar for $Pd_3Fe(111)$. The Pt(111) crystal was annealed at 1500 K, using induction heating. The crystals, protected by a droplet of Milli-Q water, immediately were transferred into an electrochemical cell and immersed in 0.1 M $HClO_4$ (Optima, Fisher Scientific) under potential control. Irrespective of the initial potentials, the first scans, as well as the subsequent anodic scans, did not exhibit any features attributable to Fe dissolution from the annealed $Pd_3Fe(111)$ surface. We observed an Fe dissolution peak in the nonannealed $Pd_3Fe(111)$. For the ORR measurements, the crystals were mounted in a rotating ring-disk assembly (Pine Instrument) after voltammetric characterization, and after we had deposited a Pt monolayer via underpotential deposition (UPD) to replace the Cu monolayer. Details of the galvanic replacement of Cu UPD adlayer by Pt were reported elsewhere.[5] All specific

(9) Adzic, R. R. DOE Hydrogen and Fuel Cell Review Meeting; Philadephia, PA, 2004.
(10) Shao, M. H.; Huang, T.; Liu, P.; Zhang, J.; Sasaki, K.; Vukmirovic, M. B.; Adzic, R. R. *Langmuir* **2006**, *22*, 10409.
(11) Shao, M. H.; Sasaki, K.; Adzic, R. R. *J. Am. Chem. Soc.* **2006**, *128*, 3526.
(12) Shao, M. H.; Sasaki, K.; Liu, P.; Adzic, R. R. *Z. Phys. Chem.* **2007**, *221*, 1175.
(13) Fernández, J. L.; Raghuveer, V.; Manthiram, A.; Bard, A. J. *J. Am. Chem. Soc.* **2005**, *127*, 13100.
(14) Fernandez, J. L.; White, J. M.; Sun, Y.; Tang, W.; Henkelman, G.; Bard, A. J. *Langmuir* **2006**, *22*, 10426.
(15) Mustain, W. E.; Kepler, K.; Prakash, J. *Electrochim. Acta* **2007**, *52*, 2102.
(16) Masahiro, W.; Kazunori, T.; Takayuki, M.; Toshihide, N.; Paul, S. *J. Electrochem. Soc.* **1994**, *141*, 2659.
(17) Shao, M.; Liu, P.; Zhang, J.; Adzic, R. *J. Phys. Chem. B* **2007**, *111*, 6772.
(18) Zhou, W.-P.; Vukmirovic, M.; Sasaki, K.; Adzic, R. *ECS Trans.* **2008**, *13*, 23.
(19) Suo, Y.; Zhuang, L.; Lu, J. *Angew. Chem., Int. Ed.* **2007**, *46*, 2862.
(20) Derry, G. N.; McVey, C. B.; Rous, P. J. *Surf. Sci.* **1995**, *326*, 59.
(21) Mousa, M. S.; Loboda-Cackovic, J.; Block, J. H. *Vacuum* **1995**, *46*, 117.
(22) Michel, A. C.; Lianos, L.; Rousset, J. L.; Delichère, P.; Prakash, N. S.; Massardier, J.; Jugnet, Y.; Bertolini, J. C. *Surf. Sci.* **1998**, *416*, 288.
(23) Nilekar, A. U.; Ruban, A. V.; Mavrikakis, M. *Surf. Sci.* **2009**, *603*, 91.
(24) Ruban, A. V.; Skriver, H. L.; Nørskov, J. K. *Phys. Rev. B* **1999**, *59*, 15990.
(25) Kampshoff, E.; Hahn, E.; Kern, K. *Phys. Rev. Lett.* **1994**, *73*, 704.
(26) Rodriguez, J. A. *Surf. Sci. Rep.* **1996**, *24*, 223.
(27) Rodriguez, J. A. *Prog. Surf. Sci.* **2006**, *81*, 141.
(28) Adzic, R. R. In *Encyclopedia of Electrochemistry*; Bard, A. J., Stratmann, M., Eds.; Wiley-VCH: Weinheim, Germany, 2002.
(29) Kibler, L. A.; El-Aziz, A. M.; Hoyer, R.; Kolb, D. M. *Angew. Chem., Int. Ed.* **2005**, *44*, 2080.
(30) Rodriguez, J. A.; Goodman, D. W. *Acc. Chem. Res.* **1995**, *28*, 477.
(31) Zhou, W. P.; Lewera, A.; Bagus, P. S.; Wieckowski, A. *J. Phys. Chem. C* **2007**, *111*, 13490.
(32) Kitchin, J. R.; Nørskov, J. K.; Barteau, M. A.; Chen, J. G. *Phys. Rev. Lett.* **2004**, *93*, 156801.
(33) Alayoglu, S.; Nilekar, A. U.; Mavrikakis, M.; Eichhorn, B. *Nat. Mater.* **2008**, *7*, 333.
(34) Greeley, J.; Jaramillo, T. F.; Bonde, J.; Chorkendorff, I. B.; Norskov, J. K. *Nat. Mater.* **2006**, *5*, 909.
(35) Mavrikakis, M.; Hammer, B.; Nørskov, J. K. *Phys. Rev. Lett.* **1998**, *81*, 2819.
(36) Jerdev, D. I.; Koel, B. E. *Surf. Sci.* **2002**, *513*, L391.

activities were calculated using the geometric surface area. For our discussions, we consider only the ORR curves obtained in a positive sweep direction.

The kinetic current for the ORR is derived from the Koutecký−Levich equation (eq 1):

$$j = \left(\frac{1}{j_k} + \frac{1}{j_D}\right) = \left(\frac{1}{j_k} + \frac{1}{B\omega^{1/2}}\right) \quad (1)$$

where j is the measured disk current density; j_k and j_D are the kinetic and diffusion current densities, respectively; B is a constant; and ω is the rotation speed. The experimental value for factor B, 0.136 mA $s^{-1/2}$, agrees well with the theoretical value of 0.143 mA $s^{-1/2}$ calculated for a four-electron-reduction process. The calculation of the B factor ($B = 0.62nFAD_{O_2}{}^{2/3}\nu^{-1/6}C_{O_2}$) was based on published values for the diffusion coefficient of O_2 ($D_{O_2} = 1.93 \times 10^{-5}$ cm^2 s^{-1}),[37] the kinetic viscosity of the solution ν ($\nu = 1.009 \times 10^{-2}$ cm^2 s^{-1}),[38] the concentration of dissolved O_2 in solution ($C_{O_2} = 1.26 \times 10^{-3}$ mol L^{-1}),[38] the Faraday constant (F), and the electrode's geometric area (A).

For voltammetry measurements, we used the standard three-electrode electrochemical cell with a Pt-foil counter electrode. The reference electrode was Ag/AgCl/KCl(3M) separated by a bridge from the reference compartment; however, all potentials are quoted with respect to a reversible hydrogen electrode (RHE). In the ring-disk measurements, the ring electrode was potentiostated at 1.28 V to maintain the peroxide oxidation reaction under pure diffusion control. Before each ORR measurement, the solution was purged with high-purity oxygen gas (Matheson, 99.9999%) for at least 40 min to ensure the oxygen saturation.

2.3. DFT Calculations. Periodic self-consistent PW91-GGA DFT calculations were performed with DACAPO[39,40] to calculate binding energies of O, OH, OOH, H_2O_2, and H_2O and the activation-energy barriers for all the ORR-relevant bond-making/breaking steps for three possible reaction mechanisms, whereby the O−O bond is broken before any, or one, or two H additions to O_2. Voltage-bias corrections were implemented according to Nørskov et.al.'s scheme.[41] Nilekar and Mavrikakis provide technical details of these calculations elsewhere.[42]

3. Results

3.1. UHV Characterization of $Pd_3Fe(111)$ Electrode. Figure 1 shows the LEIS spectra for a clean $Pd_3Fe(111)$ after annealing to various temperatures. We determined the composition of the surface layer of the annealed $Pd_3Fe(111)$ using LEIS.[36] The resulting data show that the atomic fraction of Pd at the outmost layer increases as a function of the annealing temperature, from the initial 75 atom % (i.e., bulk composition) at room temperature, to more than 90 atom % at 1200 K. The well-ordered surface of the crystals annealed at 1200 K is denoted by the (1 × 1) LEED pattern (i.e., that of bulk termination) with sharp spots in the inset in Figure 1. Stamenkovic et al.[43] investigated the dissolution of Co and Ni from the surface of a Pt−M alloy (M = Co, Ni) in acid environments; they found that Co on the topmost layer instantly dissolves, even when the PtCo surface was just rinsed with 0.1 M $HClO_4$. However, when our annealed $Pd_3Fe(111)$ electrode was treated with 0.1 M $HClO_4$, apparently only a small amount, if any, of Fe in the topmost layer immediately dissolved since no voltammetric features related to Fe dissolution were observed, leaving a pure Pd skinlike layer on the surface (referred to hereafter as Pd/annealed-$Pd_3Fe(111)$) and verifying the migration of Pd to the surface during annealing.

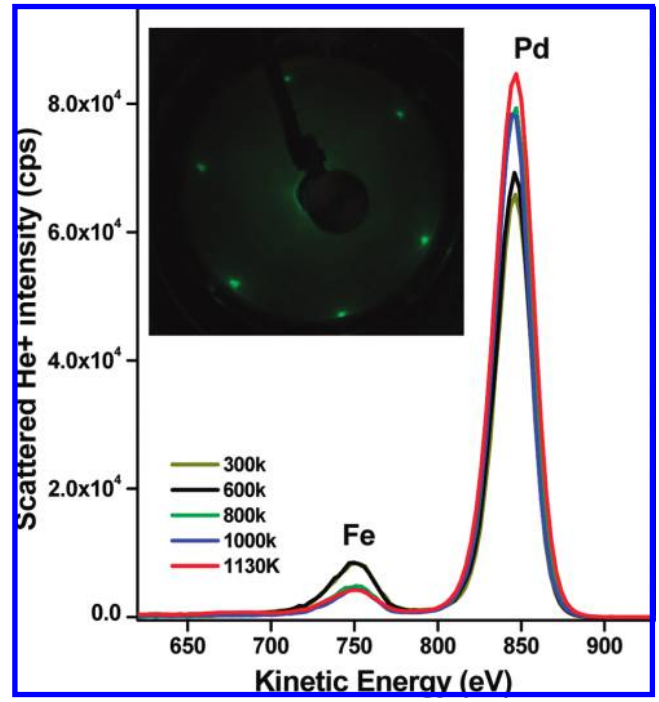

Figure 1. LEIS spectra (1 keV He^+) for a $Pd_3Fe(111)$ surface annealed to various temperatures. Inset shows a (1 × 1) LEED pattern for a $Pd_3Fe(111)$ surface annealed to 1200 K. The electron beam energy was 55 eV.

3.2. ORR Kinetics on $Pd_3Fe(111)$. Figure 2a shows the cyclic voltammetry scans for a Pd/annealed-$Pd_3Fe(111)$ surface immersed in 0.1 M $HClO_4$ at 0.05 V and subsequently cycled between 0.05 V and various positive potential limits at a scan rate of 20 mV s^{-1}. A reversible process is observed between +0.05 and +0.40 V, having a charge density of 215 ± 5 μC cm^{-2} after double-layer correction, a finding that has not been reported previously for a Pd(111) electrode (Figure 2b).[44,45] Baldauf and Kolb[46] reported that H absorption (H_{abs}) occurs only for Pd films thicker than 2 ML. This reversible process that is very similar to the $H_{ads/des}$ occurred on a Pd_{ML}/Pt(111) electrode[47] and therefore is tentatively assigned to $H_{ads/des}$ on a segregated Pd layer on a $Pd_3Fe(111)$ surface. The surface oxidation of a Pd/annealed-$Pd_3Fe(111)$ electrode does not occur until the positive potential limit extends beyond 0.73 V (red and blue line in Figure 2a); this indicates the positively shifted onset of oxidation of ~0.1 V relative to that of Pd(111). The charge density under the cathodic peak at ~0.73 V, reflecting the surface coverage of oxygen-containing species, is considerably smaller for the Pd/annealed-$Pd_3Fe(111)$ electrode than for

(37) Anastasijevic, N. A.; Vesovic, V.; Adzic, R. R. *J. Electroanal. Chem.* **1987**, *229*, 317.
(38) *CRC Handbook of Chemistry and Physics*, 75th ed.; Lide, D. R., Ed.; CRC Press: Boca Raton, FL, 1995.
(39) Greeley, J.; Nørskov, J. K.; Mavrikakis, M. *Annu. Rev. Phys. Chem.* **2002**, *53*, 319.
(40) Hammer, B.; Hansen, L. B.; Nørskov, J. K. *Phys. Rev. B* **1999**, *59*, 7413.
(41) Norskov, J. K.; Rossmeisl, J.; Logadottir, A.; Lindqvist, L.; Kitchin, J. R.; Bligaard, T.; Jonsson, H. *J. Phys. Chem. B* **2004**, *108*, 17886.
(42) Nilekar, A. U.; Mavrikakis, M. *Surf. Sci.* **2008**, *602*, L89.
(43) Stamenkovic, V. R.; Mun, B. S.; Mayrhofer, K. J. J.; Ross, P. N.; Markovic, N. M. *J. Am. Chem. Soc.* **2006**, *128*, 8813.
(44) Hoshi, N.; Kagaya, K.; Hori, Y. *J. Electroanal. Chem.* **2000**, *485*, 55.
(45) Hoshi, N.; Kuroda, M.; Hori, Y. *J. Electroanal. Chem.* **2002**, *521*, 155.
(46) Baldauf, M.; Kolb, D. M. *Electrochim. Acta* **1993**, *38*, 2145.
(47) Arenz, M.; Stamenkovic, V.; Schmidt, T. J.; Wandelt, K.; Ross, P. N.; Markovic, N. M. *Surf. Sci.* **2002**, *506*, 287.

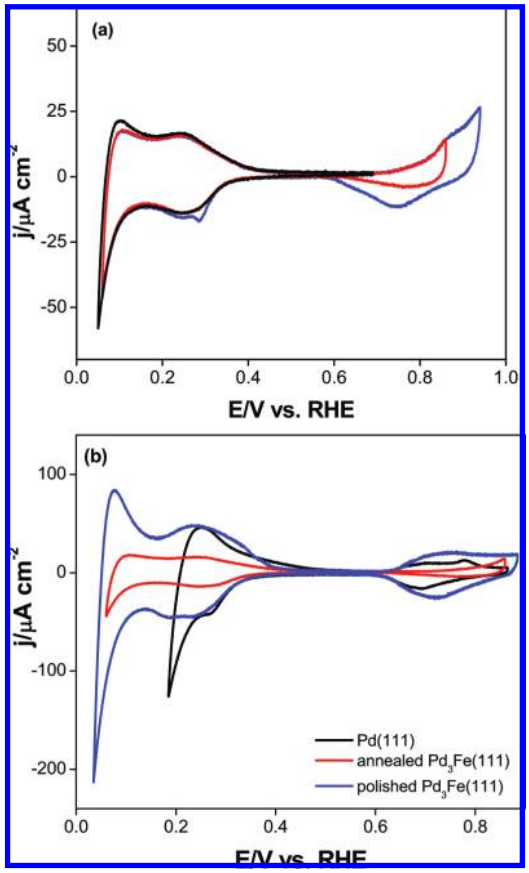

Figure 2. (a) Voltammetry curves for an annealed $Pd_3Fe(111)$ in 0.1 M $HClO_4$ solution with different positive potential windows. (b) Voltammetry curves for an annealed (red line) and a polished $Pd_3Fe(111)$ (blue line), and Pd(111) (black line) in 0.1 M $HClO_4$ solution. Scan rate: 20 mV s^{-1}.

the Pd(111) one (Figure 2b). These important new properties of the alloy's surface play a role in determining the kinetics of the ORR. A similar electrochemical phenomenon occurred on a Pt skin surface on Pt_3Ni alloys.[48,49] The voltammetry curves stayed unchanged, even after driving the positive potential limit very high (i.e., 0.95 V). However, a small peak appeared at 0.28 V in a cathodic sweep after large numbers of cycles between 0.05 and 0.95 V, which could be due to defects generated by multicycles of surface reduction and oxidation.

To assess the role of Fe in determining the electrochemical and catalytic properties of the Pd layer on the $Pd_3Fe(111)$ surface, the $Pd_3Fe(111)$ electrode was mechanically polished and its potential cycled 60 times between 0.05 and 1.3 V in 0.1 M $HClO_4$. In this way, it is very likely that the Fe atoms in several topmost layers were removed almost completely. The remaining Pd layers on the $Pd_3Fe(111)$ electrode (referred to as Pd/polished-$Pd_3Fe(111)$ hereafter) have some similarity to the Pt_3Ni skeleton surface described by Stamenkovic et al.,[43] except this pure Pd surface layer likely was thicker, as inferred from the intensive conditions for Fe dissolution we applied. For comparison, the cyclic voltammetry for a Pd/polished-$Pd_3Fe(111)$ electrode in 0.1 M $HClO_4$ is plotted in Figure 2b (blue line). The different electrochemical behavior of these three

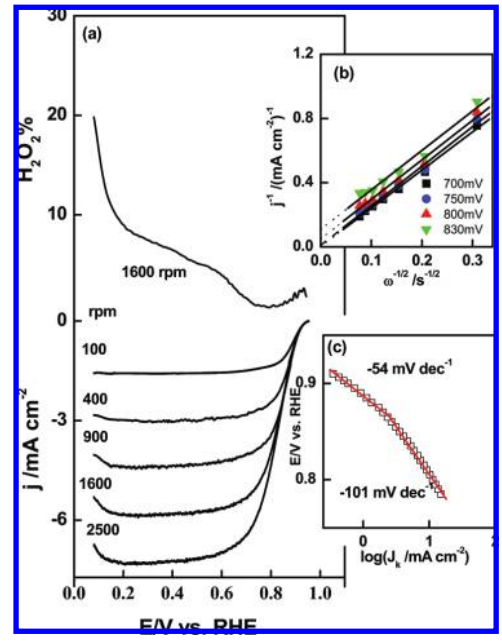

Figure 3. (a) Polarization curves of disk (j_D) (lower panel) and fraction of H_2O_2 production detected on ring (upper panel) for the ORR on the annealed $Pd_3Fe(111)$ surface in oxygen-saturated 0.1 M $HClO_4$ at room temperature; ring potential: 1.28 V; ring and disk areas are 0.126 and 0.307 cm^2, respectively; collection efficiency: $N = 0.245$, scan rate: 20 mV s^{-1}. (b) Koutecký−Levich plot at various potentials. (c) Tafel plot at 1600 rpm.

surfaces is evident. The Pd/polished-$Pd_3Fe(111)$ electrode showed very similar electrochemical behavior to that of a Pd(111) electrode (i.e., almost the same onset potentials for $H_{ad/des}$ and surface-oxide formation/reduction ($Oxide_{form/red}$)), except that the $H_{ad/des}$ process still was clearly separated from the process of hydrogen absorption and/or evolution. The charge densities for the $H_{ad/des}$ and $Oxide_{form/red}$ processes on the Pd/polished-$Pd_3Fe(111)$ electrode were considerably larger than those on the Pd/annealed-$Pd_3Fe(111)$ electrode because of the latter's high surface roughness.

Figure 3 illustrates (a) a set of polarization curves for the ORR on Pd/annealed-$Pd_3Fe(111)$ in 0.1 M $HClO_4$ at room temperature, (b) the Koutecký−Levich plots, and (c) the diffusion-corrected Tafel plot. The polarization curves have two characteristic regions: The well-defined limiting currents (j_D) region (0.2−0.7 V) and the mixed diffusion-kinetic control region (0.7−0.95 V). The ring currents denote the formation of H_2O_2 during the ORR. Under typical fuel cell operating conditions, between 0.7 and 0.95 V, only a very small fraction of H_2O_2 was formed on Pd/annealed-$Pd_3Fe(111)$, indicating an almost complete process of $4e^-$ reduction in this potential region. The increase in H_2O_2 production coincided with hydrogen adsorption and reached a maximum of ~20% at 0.08 V (ref 46 details the calculation of the fraction of H_2O_2 formation, $X_{H_2O_2}$). H_2O_2 production was independent of the rotating rates (only the 1600 rpm curve is shown here). The disk current and fraction of H_2O_2 production at subsequent cycles remained almost the same, highlighting the stability of the Pd skinlike structure during the entire ORR measurement.

Figure 3b shows the Koutecký−Levich plots whose linearity and parallelism suggest first-order kinetics with respect to molecular oxygen.[37] The diffusion-current-corrected Tafel plot is shown at Figure 3c, wherein the kinetic currents were obtained from either eq 1 (see Methods) or Figure 3b. Two Tafel slopes were observed: −54 mV dec^{-1} in the potential range of 0.91 V

(48) Stamenkovic, V.; Schmidt, T. J.; Ross, P. N.; Markovic, N. M. *J. Phys. Chem. B* **2002**, *106*, 11970.
(49) Stamenkovic, V. R.; Fowler, B.; Mun, B. S.; Wang, G. F.; Ross, P. N.; Lucas, C. A.; Markovic, N. M. *Science* **2007**, *315*, 493.

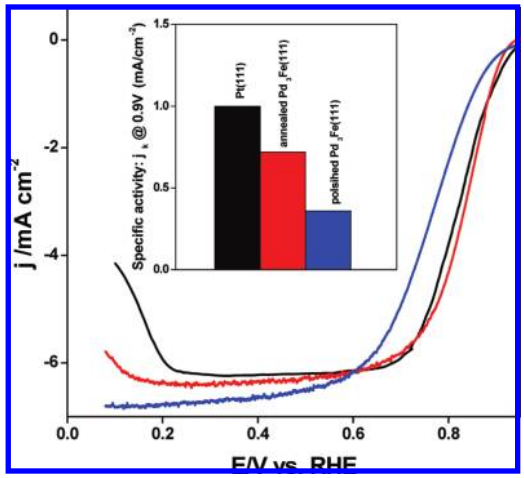

Figure 4. Polarization curves for the ORR on the annealed (red) and polished (blue) $Pd_3Fe(111)$ surfaces and also on a Pt(111) surface at 1600 rpm in oxygen-saturated 0.1 M $HClO_4$ at room temperature; scan rate: 20 mV s^{-1}. Inset shows the bar plot for the comparison of ORR specific surface activities of the corresponding three surfaces at 0.9 V_{RHE}.

$> E >$ 0.87 V and -101 mV dec^{-1} in the potential range of 0.86 V $> E >$ 0.75 V. Two Tafel slopes were also reported for Pt(111),[50] for a Pd-monolayer-covered Pt(111)[10] electrode and for a Pt skin on $Pt_3Ni(111)$[48] in 0.1 M $HClO_4$ solution. Wang et al.[50] recently ascribed the two Tafel slopes for Pt(111) in $HClO_4$ solution to the blocking and/or the electronic effect caused by a change in the coverage of the adsorbed oxygen-containing species with alterations in the potential.

Figure 4 illustrates a set of polarization curves for the ORR on Pt(111) and for annealed and polished $Pd_3Fe(111)$ electrodes in 0.1 M $HClO_4$ at room temperature. The inset shows the corresponding specific activity at 0.9 V. The Pd/annealed-$Pd_3Fe(111)$ surface shows ORR activity comparable to that of a Pt(111) surface and has nearly double the ORR activity of the polished-$Pd_3Fe(111)$ surface, even though the latter has a larger surface area.

3.3. ORR Kinetics on a Pt Monolayer-Covered $Pd_3Fe(111)$. Figure 5a shows the voltammetry curves for the UPD of Cu on a Pd/annealed-$Pd_3Fe(111)$ electrode (blue line), revealing one pair of sharp reversible peaks at around 0.52 V. The behavior of Cu on this surface is very similar to its behavior on a Pd(111) surface.[5,51] The red line represents a Pd/annealed-$Pd_3Fe(111)$ electrode in a Cu-free solution. The Cu UPD charge density is ~410 μC cm^{-2} (i.e., quite close to that of a complete pseudomorphic Cu adlayer on a Pd/annealed-$Pd_3Fe(111)$ electrode calculated using the measured $H_{ads/des}$ charge density of 215 μC cm^{-2}). Subsequently, we rinsed the Pd/annealed-$Pd_3Fe(111)$ electrode covered with this monolayer of Cu with deaerated water to remove the attached Cu^{2+} solution and reimmersed the electrode in a solution of 1 mM K_2PtCl_4 + 50 mM H_2SO_4 at open circuit potential for three minutes.[5] From their STM studies, Zhang et al.[5] reported observing a Pt_{ML} consisting of monatomic height islands on Pd(111), prepared by the same method.

Figure 5b shows the voltammetry curves for the Pt_{ML} on the Pd/annealed-$Pd_3Fe(111)$ electrode (referred to as Pt_{ML}/Pd/annealed-$Pd_3Fe(111)$) prepared by this Cu replacement method

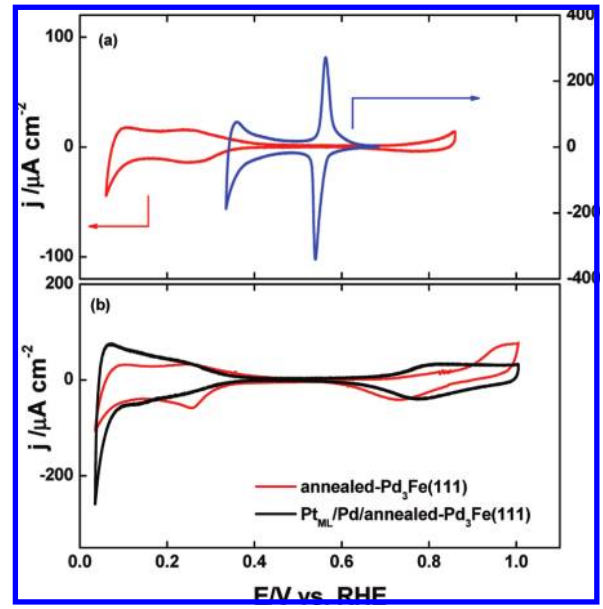

Figure 5. (a) Voltammetry curves for the under-potential deposition of Cu (blue line) on a $Pd_3Fe(111)$ electrode in 0.05 M H_2SO_4 with 0.05 M $CuSO_4$, and also for the $Pd_3Fe(111)$ surface in 0.1 M $HClO_4$ solution lacking Cu^{2+} (red line); scan rate: 20 mV s^{-1}. (b) Voltammetry curves for a Pt monolayer (ML) covering a $Pd_3Fe(111)$ surface (black line) obtained by galvanic replacement of the Cu monolayer from Figure 5a and for a $Pd_3Fe(111)$ surface in 0.1 M $HClO_4$ solution (red line). Scan rate: 50 mV s^{-1}.

(black line) and also the Pd/annealed-$Pd_3Fe(111)$ electrode (red line) in 0.1 M $HClO_4$. The presence of a Pt monolayer causes changes in both H adsorption and surface oxidation features. The hydrogen adsorption/desorption charge for the Pt_{ML}/Pd/annealed-$Pd_3Fe(111)$ was 240 $\pm$ 15 μC cm^{-2} after double-layer correction. Interestingly, the hydrogen evolution from this Pt_{ML}/Pd/$Pd_3Fe(111)$ surface occurred at more positive potential than that on the surface of Pd/annealed-$Pd_3Fe(111)$.

Figure 6 shows the ORR results for a Pt_{ML}/Pd/annealed-$Pd_3Fe(111)$ electrode in 0.1 M $HClO_4$ at room temperature. An important property of the electrode's surface is the almost complete elimination of H_2O_2 formation between 0.08 and 1.04 V (Figure 6a). The maximum H_2O_2 amount calculated from the measured ring current is less than 1% at 0.08 V, suggesting a complete four-electron reduction process throughout this wide range of potential. Figure 6c also shows two Tafel slopes, -78 and -108 mV dec^{-1}, respectively, for the potential range of 0.96 V $> E >$ 0.87 V and 0.86 V $>$ E $>$ 0.75 V. The similar Tafel slopes obtained for the ORR on the surfaces of Pt_{ML}/Pd/$Pd_3Fe(111)$, Pd/$Pd_3Fe(111)$, Pt(111),[50] and $Pt_3Ni(111)$[48] suggest a similar reaction pathway on those.

Figure 7a provides a set of polarization curves for the ORR on the Pt_{ML}-covered surfaces of Pd/annealed-$Pd_3Fe(111)$ and Pd(111), and Pt(111) obtained in 0.1 M $HClO_4$ at room temperature. Figure 7b has their corresponding specific activities at 0.9 V. A Pt monolayer supported on Pd/annealed-$Pd_3Fe(111)$ shows the highest ORR kinetics among these three surfaces, by a factor of at least 2 compared with that of the Pt(111) surface, and also demonstrates significantly increased ORR activity in comparison with that of the Pt_{ML}/Pd(111) surface.

4. Discussion

Changes in the electronic properties of segregation-induced Pd alloy surfaces have not been studied with single-crystal surfaces in an electrocatalytic environment, except in our

(50) Wang, J. X.; Markovic, N. M.; Adzic, R. R. *J. Phys. Chem. B* **2004**, *108*, 4127.
(51) Cuesta, A.; Kibler, L. A.; Kolb, D. M. *J. Electroanal. Chem.* **1999**, *466*, 165.

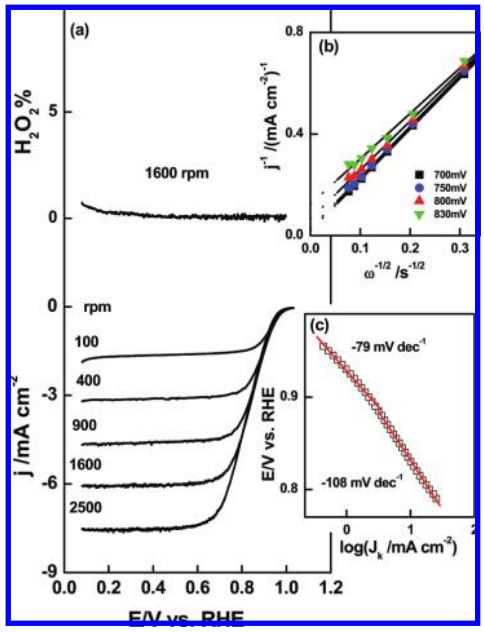

Figure 6. (a) Polarization curves of disk (*j*) (lower panel) and fraction of H_2O_2 production (upper panel) detected on ring (anodic sweep direction) for the ORR on the Pt monolayer covered $Pd_3Fe(111)$ surface in oxygen-saturated 0.1 M $HClO_4$ at room temperature; ring potential: 1.28 V; ring and disk areas are 0.126 and 0.307 cm^2, respectively; collection efficiency: $N = 0.245$; scan rate: 20 mV s^{-1}. (b) Koutecký−Levich plot at various potentials. (c) Tafel plot at 1600 rpm.

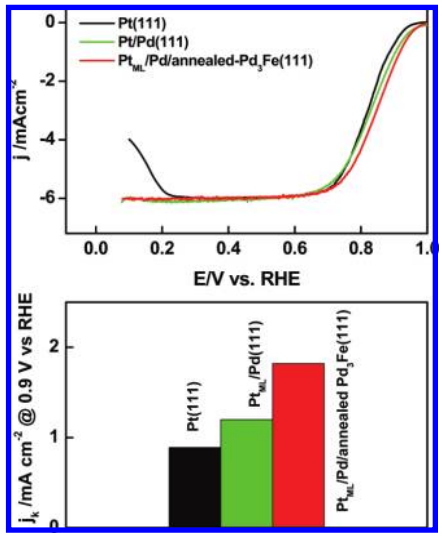

Figure 7. (a) Polarization curves for the ORR on a Pt monolayer covered annealed-$Pd_3Fe(111)$ (red), annealed-Pd(111) (green), and Pt(111) surfaces (black) at 1600 rpm in oxygen-saturated 0.1 M $HClO_4$ at room temperature; scan rate: 20 mV s^{-1}. Inset shows the bar plot for the comparison of ORR specific activities of the corresponding three surfaces at 0.9 V_{RHE}.

preliminary report.[18] Pd−M alloys (M = Co, Fe, or Ti)[9−16,18] have shown comparable or slightly better ORR activity than commercial Pt catalysts. The high ORR kinetics and significantly decreased cost of materials along with their satisfactory stability make some Pd−M alloys very promising candidates to replace conventional Pt catalysts for the ORR. The enhanced ORR activity observed with bulk and high-surface-area Pd−M alloys was ascribed either to the modification of the electronic property of Pd on the segregated surface layer[9,11,17,18] or to the synergistic effect between Pd and the second metal.[13−15] This study involving the well-ordered $Pd_3Fe(111)$ single-crystal surface provides fundamental information on the role of surface properties of Pd alloys in the ORR kinetics that was previously unattainable.

As demonstrated in our ex situ UHV studies (Figure 1), a layer of pure Pd is formed on the high-temperature-annealed $Pd_3Fe(111)$ electrode, suggesting the high tendency of Pd to segregate to the surface in a Pd−Fe alloy system, in good agreement with theoretical predictions.[24] Pd segregation on the surface of Pd−M (M = Co, Ni, Cu) alloys also was reported in some UHV studies.[20−22] Our LEED study (inset in Figure 1) confirmed that the bulk termination of a $Pd_3Fe(111)$ single crystal extended into the segregated Pd surface layer (i.e., (1 × 1) LEED pattern). This Pd/annealed-$Pd_3Fe(111)$ surface, however, showed a very different electrochemical (Figure 2) and electrocatalytic (Figure 4) behavior compared with the Pd(111) and the Pd/polished-$Pd_3Fe(111)$ surfaces.

On the basis of DFT calculations, Shao et al.[17] reported a downshift (∼0.25 eV) of the d-band center of the Pd skin on $Pd_3Fe(111)$ with respect to Pd(111); they assigned it to a combination of compressive strain and electron redistribution between the Pd skin and subsurface layers (ligand effect[52,53]). Nørskov et al.[35,54] indicated that changes in adsorption energies for reactions are directly linked to changes in position of the metal/alloy d-band center with respect to the Fermi level. Therefore, we might expect that a downshift in the Pd d-band center decreases the interaction of oxygen or oxygen-containing species with Pd (i.e., lowers the bond strength between Pd and oxygen-containing species (BE_{Pd-O})) and, hence, decreases the respective species surface coverage. It is generally believed that the ORR kinetics on Pd is limited by the rate of removal of adsorbed oxygen-containing species (i.e., the bulk Pd surface binds the ORR intermediates too strongly and as a result experiences a hindered rate of O or OH removal through protonation).[2,17] Both effects will cause the buildup of the O or OH surface coverage that blocks O_2 adsorption and dissociation sites. A downshift of the Pd d-band center that may weaken the Pd−O and/or Pd−OH bond strength might also facilitate the O/OH removal through protonation rates. In turn, this may increase the available Pd sites for O_2 adsorption and dissociation and, hence, increase the ORR activity. Voltammetry shows a positive shift of the onset of the surface oxidation for a Pd/annealed-$Pd_3Fe(111)$ electrode and reduced surface oxide coverage relative to a Pd(111) surface (Figure 2). This surface has ORR kinetics comparable to a Pt(111) surface (Figure 4). Both results are in accord with the theoretical predictions for the electronic and chemical properties of the Pd skin on $Pd_3Fe(111)$.[17] Similarly, a downshift of the d-band center, caused by the effects of subsurface Ni or Co, and an enhanced ORR activity were reported for a Pt layer formed on $Pt_3Ni(111)$[49] and $Pt_3Co(111)$[43] electrodes.

For high-surface-area Pd−M or Pt−M (M = 3d transition metals) alloy catalysts, the surface is unstable in acidic environment and 3d transition metals tend to leach out, resulting in an increased surface area enriched with noble metals that, as was argued above, is responsible for the enhanced ORR activity on these supported catalysts.[55,56] For practical applications of the Pd_3Fe catalyst, the effect of surface and subsurface Fe dissolution on the ORR is important. The very rough surface of $Pd_3Fe(111)$ after exposure to 60 cycles with a positive potential

(52) Greeley, J.; Mavrikakis, M. *Nat. Mater.* **2004**, *3*, 810.
(53) Xu, Y.; Ruban, A. V.; Mavrikakis, M. *J. Am. Chem. Soc.* **2004**, *126*, 4717.
(54) Hammer, B.; Nørskov, J. K. *Adv. Catal.* **2000**, *45*, 71.

limit of 1.3 V was caused by the dissolution of Fe atoms from the several topmost layers, as inferred from the voltammetry curves (Figure 2). The ORR kinetics on this Pd/polished-$Pd_3Fe(111)$ surface was a factor of 2 lower than that of the Pd/annealed-$Pd_3Fe(111)$ surface (Figure 4). As expected, the electronic properties of a Pd skin on $Pd_3Fe(111)$ surface gradually approached those of Pd bulk following the subsurface Fe dissolution, because with this subsurface depletion the ligand effect and/or compressive strain[7,30−33,35] from Fe to Pd eventually disappear. The fact that the electronic properties of the Pd skin gradually approach those of Pd bulk is reflected on its catalytic activity, as demonstrated from our ORR studies. In addition to this electronic property change, disordering (roughening) of the surface structure could partly be responsible for the loss of ORR activity.[2,43] Thus, the catalytic activity of Pd−M alloys for the ORR appears to be determined not only by the alloying elements, but also by the distribution of Pd and Fe atoms in the near-surface region, the surface's geometry, and its morphology.

Thus far, we demonstrated that the Pd/annealed-$Pd_3Fe(111)$ surface shows ORR activity comparable to that of a Pt(111) electrode, so it could be a very interesting material candidate for replacing conventional Pt catalysts for ORR. However, we also found that the ORR activity of Pd_3Fe alloy decreased when Fe leached out. Since Pd has lower dissolution potential than Pt, 0.98 V vs 1.07 V in 1 M H_2SO_4,[57] adding one more layer, such as Pt, to protect the Pd_3Fe alloy from Fe dissolution would preserve the unique surface property of Pd alloy materials, which is critical for its eventual use as the ORR catalyst in PEMFCs.

As indicated in the Introduction, one motivation of our work was to gain further understanding of the Pt_{ML}−substrate interaction, the key factor determining the electrocatalytic activity of a Pt_{ML}. We demonstrated previously[4,5] that a Pt_{ML} deposited on a Pd(111) surface has higher ORR kinetics than Pt(111). Furthermore, metal monolayers supported on different substrates can exhibit chemical and catalytic properties very different from those of the surfaces of individual metals.[4,25−29,33,34] A good correlation between the activity and the calculated (DFT) d-band center shift for a Pt_{ML} on six substrates strongly suggests that the changes in the electronic properties of Pt_{ML}, caused by Pt_{ML}−substrate interaction, generate this increase in activity.[7,30−32,54,58] The activity d-band center dependence produced a volcano-type plot with the Pt_{ML} on Pd substrate on top of it.[4] It is of fundamental and practical importance to understand whether the ORR activity of a Pt_{ML} can be further increased, since these catalysts offer a very attractive approach for resolving the problems of high Pt content and low efficiency apparent in conventional Pt electrocatalysts.[4,7] The fine-tuning approach described in this work that involves the Pt_{ML}−Pd interaction further tuned by Pd alloyed with Fe in Pd_3Fe offers an effective procedure. We showed in this study that the surface Pd layer formed on high-temperature-annealed $Pd_3Fe(111)$ has the same surface structure as the Pd(111) surface, but somewhat different electronic properties (i.e., a −0.25 eV downshift of the d-band center[17]) making the $Pd_3Fe(111)$ crystal a suitable substrate to study the Pt_{ML} fine-tuning approach.

Table 1. Binding Energies of OH on the Surfaces of Pt(111), Pt_{ML}/Pd(111), and Pt_{ML}/Pd/Pd_3Fe(111)

	Pt(111)	Pt_{ML}/Pd(111)	Pt_{ML}/Pd/Pd_3Fe(111)
BE_{OH} (eV)	−2.09	−2.07	−1.93

To elucidate the fundamental aspects of the ORR activity of composite core−shell structures, DFT calculations[59] were conducted for model systems composed of a single Pt_{ML} on a Pd monolayer supported on the close-packed surfaces of several different substrates. On the basis of this analysis, the binding energy of OH on Pt_{ML}/Pd(111) is weaker than that of OH on Pt(111) and OH removal is easier on Pt_{ML}/Pd(111) than it is on Pt(111) (Table 1). As a result, the ORR activity is increased on Pt_{ML}/Pd(111) compared to that on Pt(111). As shown in Table 1, in Pt_{ML}/Pd/$Pd_3Fe(111)$, which is an appropriate model for the Pt_{ML} on the Pd/annealed-$Pd_3Fe(111)$ surface, the binding of OH is destabilized much more so than the destabilization between Pt_{ML}/Pd(111) and Pt(111). This leads to Pt_{ML}/Pd/$Pd_3Fe(111)$ having more OH-free sites for O_2 adsorption and reactions than the Pt_{ML}/Pd(111) and Pt(111) surfaces. Interestingly, we are finding that the activity of Pt_{ML}/Pd(111) and Pt(111) is limited by OH removal (left side of the ORR activity volcano plotted against BE_{OH}),[59] whereas the activity of Pt_{ML}/Pd/$Pd_3Fe(111)$ is limited by the O−O bond scission in the OOH intermediate, placing this surface on the other side of the volcano plot. Yet, a direct comparison between the BE_{OH} and the calculated ORR activities on Pt_{ML}/Pd(111) and Pt_{ML}/Pd/$Pd_3Fe(111)$ at the relevant bias voltage suggests that the enhanced activity of the latter surface originates mainly from the destabilization of OH on that surface, compared to that on the former surface.

5. Conclusions

We demonstrated the great potential for designing electrocatalysts with alloy nanoparticles used as cores for Pt monolayer catalysts and a possibility of modifying their activity by tuning the Pt monolayer-supporting nanoparticle interactions. For a $Pd_3Fe(111)$ alloy, a Pd layer segregated by annealing at high temperature shows the same surface structure as the Pd(111) surface but somewhat different electronic properties (i.e., −0.25 eV downshift of the d-band center compared to Pt(111)). This segregated Pd layer has ORR kinetics comparable to that of Pt(111). The high activity of the Pd layer is ascribed to the modification of the Pd surface's electronic properties by subsurface Fe. This is in agreement with directly relating the position of the d-band center to adsorption energies according to the d-band center theory of Nørskov and co-workers. The dissolution of subsurface Fe causes a drop in the ORR kinetics on Pd_3Fe. Thus, preventing the dissolution of Fe in Pd_3Fe alloys would preserve the unique surface property of Pd alloy materials, which is necessary for its use in PEMFCs. This segregated Pd layer was proven to be an excellent substrate for a Pt_{ML} ORR catalyst, as indicated by the enhanced ORR kinetics on Pt_{ML}/Pd/annealed-$Pd_3Fe(111)$ compared to that of Pt_{ML}/Pd(111) and Pt(111). Our DFT calculations indicate that this observed increase in ORR activity originates from further weakening of the Pt−OH bond. The results of this study

(55) Bruce, C. B.; Philip, N.; Ross, P. N., Jr. *J. Electrochem. Soc.* **1990**, *137*, 3368.
(56) Paffett, M. T.; Beery, J. G.; Gottesfeld, S. *J. Electrochem. Soc.* **1988**, *135*, 1431.
(57) Rand, D. A. J.; Woods, R. *J. Electroanal. Chem.* **1972**, *35*, 209.
(58) Hammer, B.; Morikawa, Y.; Nørskov, J. K. *Phys. Rev. Lett.* **1996**, *76*, 2141.
(59) Jiao, J.; Hahn, K.; Peng, G.; Adzic, R. R.; Mavrikakis, M. To be submitted for publication.

illustrate that alloying Pd with Fe causes a downshift of the Pd d-band center relative to Pd(111), which is conducive to tuning the substrate's properties and its interactions with a Pt_{ML}, which, in turn, further increases its ORR catalytic activity. Our approach seems very promising in searching for viable combinations of core−shell nanoparticles suitable for specific catalytic reaction requirements.

Acknowledgment. This work was supported by the U.S. Department of Energy, Divisions of Chemical and Material Sciences, under Contract No. DE-AC02-98CH10886. Work at UW-Madison was supported by DOE-BES. CPU time was utilized at facilities located at ANL, PNNL, ORNL, and NERSC, all supported by the DOE.

JA9039746